Lateral variation of *Lg* wave propagation in southern Mexico

Lars Ottemöller[1]
Institute of Solid Earth Physics, University of Bergen, Bergen, Norway

Nikolai M. Shapiro,[2] Shri Krishna Singh, and Javier F. Pacheco
Instituto de Geofísica, Universidad Nacional Autónoma de México, Ciudad University, Mexico City, Mexico

Received 20 September 2000; revised 30 January 2001; accepted 19 August 2001; published 17 January 2002.

[1] In this study we investigated lateral variation of *Lg* wave propagation in southern Mexico from recordings of 92 crustal earthquakes along 591 travel paths. The efficiency of *Lg* propagation was measured in terms of *Lg* to *Pn* spectral ratio. It was found that *Lg* propagation is inefficient for travel paths through the Gulf of Mexico coastal plains and the Gulf of Tehuantepec, areas with thick layers of sediments. An average *Lg* quality factor, Q_{Lg}, as a function of frequency for southern Mexico was estimated for the efficient *Lg* travel paths. The relation obtained for Q_{Lg} in the frequency range 1.6–8 Hz is $Q_{Lg}(f) = 204 f^{0.85}$. The lateral variation of Q_{Lg}^{-1} was solved as a mixed-determined inverse tomography problem, separately for each frequency, in which a spatial smoothness constraint was imposed and a priori information was added in poorly covered regions. The spatial resolution obtained was about 200 km. It was found that the Trans-Mexican Volcanic Belt, the Gulf of Mexico coastal plains, and the area east of 94°W are characterized by lower than average Q_{Lg} values, i.e., higher attenuation. High Q_{Lg} values were obtained for the Mixteco-Oaxaca terranes, while for the Guerrero terrane, values similar to the average were obtained. The results show a correlation between Q_{Lg} and crustal structure and provide valuable information on lateral variation of Q_{Lg}, which is needed for reliable prediction of ground motion during future earthquakes. *INDEX TERMS:* 7205 Seismology: Continental crust (1242), 8180 Tectonophysics: Tomography, 9350 Information Related to Geographic Region: North America

1. Introduction

[2] The tectonic structure of southern Mexico is characterized by an aggregate of several blocks that are bounded by faults. *Campa and Coney* [1983] proposed a division of southern Mexico into several tectonostratigraphic terranes (Figure 1): Xolapa, Oaxaca, Mixteco, Zapoteco, Maya, and Guerrero. The composition and tectonic evolution of these terranes were broadly explained by *Sedlock et al.* [1993]. For the purpose of the present work we differentiate between two types of terranes, those with cratonic basement such as the Oaxaca and Zapoteco terranes, and those formed from collision tectonics such as the Xolapa, Juárez, Mixteco, and Guerrero terranes. The latter terranes consist of sediments and/or oceanic rocks that collided with continental blocks and were later deformed and intruded. The Trans-Mexican Volcanic Belt (TMVB) is composed of late Miocene to present andecitic and dacitic deposits. The Gulf basin is considered to be a passive margin with a large accumulation of sediments and salt tectonics. A knowledge of the crustal and upper mantle structure in Mexico is important for understanding the tectonic evolution of this region as well as for the estimation of ground motion during future earthquakes. Since the pioneering study by *Meyer et al.* [1961] the velocity structure of the crust and upper mantle below central and southern Mexico has been the subject of numerous studies [e.g., *Fix*, 1975; *Valdés et al.*, 1986; *Gomberg and Masters*, 1988; *Nava et al.*, 1988; *Campillo et al.*, 1996; *Shapiro et al.*, 1997].

[3] The quality factor, describing attenuation of seismic waves, is one of the basic parameters characterizing Earth's crust. It depends on the type of rocks and the degree of heterogeneity and therefore is correlated with the geological structure. Several studies of attenuation and its regional variation in southern Mexico have been carried out over the last decade. An overview of these studies and their results is given in Table 1. Figure 2 shows the regions studied in previous works. *Castro et al.* [1990] determined Q from S waves recorded at distances up to 133 km along the Guerrero subduction zone by simultaneously inverting for site response, Q, and source spectra. *Ordaz and Singh* [1992] studied source spectra and spectral attenuation of crustal events in the subduction zone recorded in Guerrero and the Valley of Mexico. They obtained a frequency-dependent quality factor, $Q(f) = 273 f^{0.66}$, which may be taken as a reference value for southern Mexico. *Castro and Munguía* [1993] found a lower quality factor for S waves above the Oaxaca subduction zone. *Castro et al.* [1994] compared results for Q from Oaxaca and Guerrero and attempted to explain the unexpected lower Q in the Oaxaca region. *Domínguez et al.* [1997] studied the regional variation of attenuation of *Lg* waves between Guerrero and Oaxaca. They used travel paths between Guerrero/Oaxaca and Veracruz at the Gulf of Mexico. *Yamamoto et al.* [1997] described the lateral variation of *Lg* coda Q in southern Mexico based on events, including subcrustal events, from the subduction zone and recorded at a single station in the Valley of Mexico. They observed a higher Q value for the Michoacan-Jalisco and Oaxaca regions as compared with Guerrero. However, they reported an even higher Q value for the volcanic belt, which seems unreasonable. More efficient propagation for paths going inland as compared with paths going parallel to the coast had been suggested by *Singh et al.* [1988]. *Cárdenas et al.* [1998] investigated these differences in attenuation between paths along and perpendicular to the coast using data

[1] Now at British Geological Survey, Edinburgh, United Kingdom.
[2] Now at Center for Imaging Earth's Interior, Department of Physics, University of Colorado, Boulder, Colorado, USA.

0148-0227/02/2001JB000206$09.00

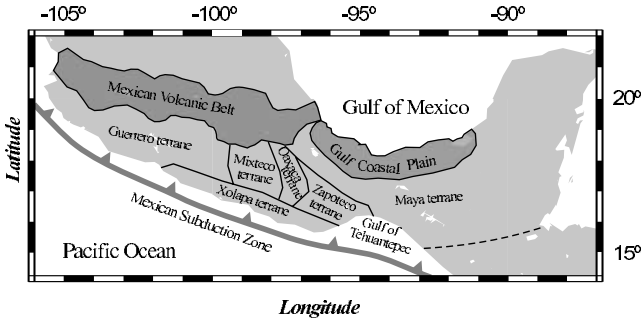

Figure 1. Main geologic units of southern Mexico.

from a seismic refraction experiment. They found lower average attenuation for the travel paths going inland.

[4] The previous Q studies for southern Mexico described local-scale attenuation based on small data sets. In southern Mexico it is possible that various tectonic provinces will be reflected in lateral variation of Q on a regional scale. We took advantage of the availability of a large, high-quality data set to study the lateral variation of Q in southern Mexico on a regional scale. This is the first study for southern Mexico that attempts to resolve regional variation of Q caused by large variations in crustal structure. Since *Lg* waves propagate in the crust and are observed over a large distance range, Q can be reliably determined from the decay of *Lg* spectral amplitudes with distance [e.g., *Campillo*, 1987; *Baumont et al.*, 1999]. The Q variation in this study is solved as a tomography problem. However, before performing a formal inversion, the efficiency of *Lg* wave propagation was quantified in terms of the spectral ratio of *Lg* to *Pn*, and an average Q value for southern Mexico was determined.

[5] The propagation of *Lg* waves as one of the dominant phases at regional distances was first described by *Press and Ewing* [1952]. The *Lg* waves have been modeled as higher-mode surface waves [*Herrmann and Kijko*, 1983] or as multiple reflected *S* waves [*Campillo et al.*, 1984; *Campillo*, 1990], which propagate in the crust. The characteristics of the propagation of *Lg* waves have been discussed for many regions [e.g., *Ruzaikin et al.*, 1977; *Campillo and Plantet*, 1991; *Campillo et al.*, 1993; *Chazalon et al.*, 1993; *McNamara et al.*, 1996; *Shi et al.*, 1996; *Benz et al.*, 1997; *Rial and Ritzwoller*, 1997; *Rodgers et al.*, 1997; *Mellors et al.*, 1999; *Calvert et al.*, 2000] and have been studied using numerical simulations [e.g., *Kennett*, 1986; *Maupin*, 1989; *Regan and Harkrider*, 1989; *Cao and Muirhead*, 1993; *Gibson and Campillo*, 1994; *Furumura and Kennett*, 1997, 1998; *Vaccari and Gregersen*, 1998]. It has been observed that *Lg* propagation becomes inefficient or is blocked if the crustal structure undergoes fast lateral changes [*Ruzaikin et al.*, 1977; *Baumgardt*, 1990; *Campillo et al.*, 1993; *Chazalon et al.*, 1993] or if the travel path crosses oceanic crust [*Press and Ewing*, 1952; *Knopoff et al.*, 1979; *Kennett et al.*, 1985; *Gregersen and Vaccari*, 1993; *Shapiro et al.*, 1996]. The lateral variation of coda Q has been determined on the basis of *Lg* coda [e.g., *Singh and Herrmann*, 1983; *Xie and Mitchell*, 1990]. Source characteristics have also been determined from the analysis of *Lg* waves [e.g., *Hasegawa*, 1983].

2. Data

[6] The network of broadband stations operated by the National Autonomous University of Mexico (UNAM) provided the high-quality, three-component broadband data used in this study. Most of the broadband seismic stations are located in southern Mexico. All stations are equipped with STS-2 sensors and a 24-bit Quanterra acquisition system, except for station TEIG, which is equipped with a Geotech KS-36000-I borehole seismometer (50-s natural period). The stations and the epicentral locations used in this study are shown in Figure 3. Seismicity is highest in the subduction zone along the Pacific coast of Mexico. *Lg* waves are most efficiently excited by earthquakes in the continental crust. Therefore only crustal earthquakes, with depths of less than 35 km, were selected from the area between 13–24°N and 94°–108°W. Locations were taken from the catalogue of the National Seismological Service (SSN). Since the depths are not well constrained, the records were visually checked for the presence of crustal phases to eliminate noncrustal events. The magnitude range was chosen between 4.5 and 6.7. An upper magnitude limit was used to avoid the effect of source complexity on the *Lg* wave propagation. It was required that the events be recorded by at least four stations. The minimum epicentral distance was set to 200 km to ensure a clear observation of *Lg* waves. The selected earthquakes were from the period October 1995 to June 2000: a total of 92 events with 591 travel paths (Figure 4). It is seen that the highest path density was obtained between the Pacific coast and central southern Mexico. The average group velocity of the *Lg* peak amplitude was found to be 3.35 km s^{-1}, and therefore the *Lg* group velocity window was selected between 3.0 and 3.7 km s^{-1}. The *Pn* group velocity window was selected between 6.5 and 8 km s^{-1}.

3. Efficiency of *Lg* Waves

[7] We characterized the efficiency of the Lg wave propagation by the spectral ratio of *Lg* to *Pn* waves. Since *Pn* propagation is less dependent on the lateral variations in the crustal structure as compared to *Lg*, this ratio provides an adequate measure of the efficiency of *Lg* propagation. Measuring the efficiency of *Lg* propagation in terms of *Lg*/*Pg* or *Lg*/*Sn* would be less valuable, since *Pg* is expected to show a similar attenuation pattern as *Lg* and *Sn* are expected to be extremely variable in volcanic regions. Contamination of *Lg* by *Sn* coda, as, for example, observed by *Shin and Herrmann* [1987] in Canada for distances larger than 500 km and frequencies above 7 Hz, was found to be negligible in Mexico.

Table 1. Overview of Results From Previous Studies of Attenuation in Southern Mexico

Reference	Type of Wave	Region	Distance Range, km	Frequency Range, Hz	Geometrical Spreading	Results
Castro et al. [1990]	*S*	Guerrero	13–133	0.1–40	$1/R$ $(1/R)^{0.5}$	$Q_S(f) = 278\, f^{0.92}$ $Q_S(f) = 96\, f^{0.96}$
Ordaz and Singh [1992]	*S*	Guerrero-Mexico City	<323	0.2–10	$1/R$ for $R \le R_x$; $(R_x R)^{-0.5}$ for $R \ge R_x$	$Q_S(f) = 273\, f^{0.66}$
Castro and Munguia [1993]	*P* and *S*	Oaxana	19–76	1.0–25	$(1/R)^{0.5}$	$Q_S(f) = 56\, f^{1.01}$ $Q_P(f) = 22 f^{0.97}$
Domínguez et al. [1997]	*Lg*	Oaxana Guerrero	285–640	2.0–7.0	$(1/R)^{0.883}$	$Q_{Lg}(f) = 59 f^{0.81}$ $Q_{Lg}(f) = 134 f^{0.83}$
Yamamoto et al. [1997]	*Lg* Coda	Oaxana Michoacan-Jalisco Guerrero	155–520	0.2–2.0		$Q_{Lg}(f) = 190 f^{0.7}$ $Q_{Lg}(f) = 195 f^{0.75}$ $Q_{Lg}(f) = 178 f^{0.65}$

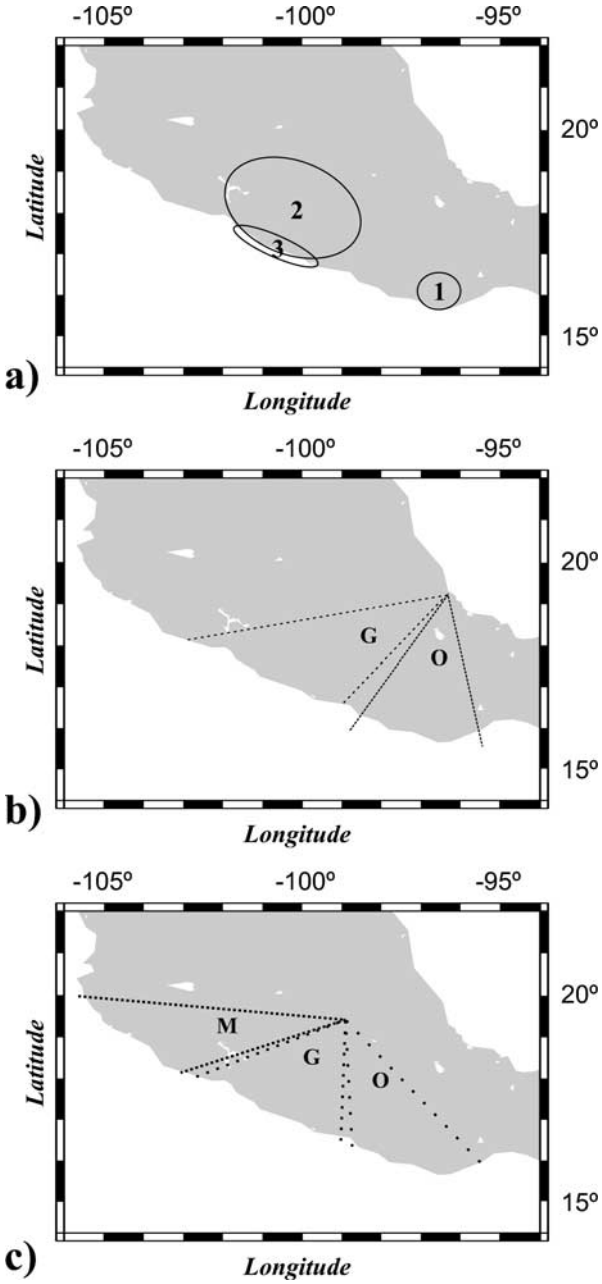

Figure 2. Regions investigated in previous *Q* studies for Mexico. (a) Area 1 studied by *Castro and Munguía* [1993], area 2 studied by *Castro et al.* [1990] and *Ordaz and Singh* [1992], and area 3 studied by *Cárdenas et al.* [1998]; (b) Guerrero (denoted by G) and Oaxaca (denoted by O) sectors studied by *Domínguez et al.* [1997]; and (c) Michoacan-Jalisco (M), Guerrero (G) and Oaxaca (O) sectors as defined by *Yamamoto et al.* [1997].

[8] For each source-receiver path the time windows corresponding to the respective group velocity windows for *Lg* and *Pn* waves were extracted, the average Fourier spectral levels around a selected center frequency were determined, and the spectral ratios of *Lg* to *Pn* waves were computed. It was required that the *Pn* spectral level be higher than twice the spectral level of the noise. We regarded an *Lg* to *Pn* ratio of below 3 as inefficient, 3 to 6 as intermediate, and above 6 as efficient. An example of efficient *Lg* propagation is shown in Figure 5. Figure 6 shows the difference between efficient and inefficient travel paths. The travel path to station TEIG, which crosses the sedimentary basin at the Gulf of Mexico shows inefficient *Lg* propagation. At lower frequencies, no *Lg* waves were seen in the seismogram for TEIG, indicating that the inefficiency is due to attenuation and not to mode conversion from *Lg* to *Sn* waves. Domination of *Sn* coda over *Lg* for this travel path toward higher frequencies was not observed.

[9] Figure 7 shows the efficiency of *Lg* wave propagation for all travel paths at 2 Hz. It is seen that all travel paths to TEIG are inefficient. Strong *Lg* attenuation can be caused by high anelastic attenuation, enhanced scattering of *S* waves, or structural effects. For example, it has been suggested that crustal thinning or strong variation of the Moho topography can result in a significant *Lg* attenuation [e.g., *Kennett*, 1986; *Campillo*, 1987; *Campillo et al.*, 1993]. *Lg* waves can also be strongly attenuated or blocked by sedimentary basins [e.g., *Knopoff et al.*, 1979; *Zhang and Lay*, 1995; *Shapiro et al.*, 1996]. In this case a large part of the *Lg* energy becomes trapped in shallow sedimentary layers where attenuation is high. We believe that the latter mechanism is responsible for the inefficient *Lg* propagation along the paths crossing large sedimentary basins, i.e., (1) the Gulf of Tehuantepec and (2) the Gulf of Mexico coastal plain [*Guzman*, 1962].

[10] It is important to note that the *Lg*/*Pn* ratio not only reflects *Lg* efficiency but also depends on the characteristics of *Pn*. In general, *Pn* is an extremely variable phase in terms of amplitude. Also, the difference between *Lg* and *Pn* in geometrical spreading and dependence on the radiation pattern will effect the *Lg*/*Pn* ratio. In spite of these difficulties the *Lg* to *Pn* spectral ratio provides a rough measure of the efficiency of *Lg* wave propagation. Figure 7 is in agreement with observations from seismograms that show *Lg* inefficiency and it is seen that lateral changes in crustal structure such as the sedimentary basin near the Gulf coast are reflected in the *Lg* propagation pattern. The *Lg*/*Pn* ratio was used as criteria to exclude inefficient paths from the determination of the average Q_{Lg}^{-1}.

4. Determination of Average Q_{Lg} in Southern Mexico

[11] The main goal of this study was to determine the lateral variation of the quality factor Q_{Lg}. However, for practical purposes of estimating ground motion and to provide an a priori estimate of Q_{Lg}, we first determined an average quality factor for southern Mexico.

[12] The *Lg* wave displacement spectral amplitude $A_{kl}(f)$ for the event k, at the recording site l, after removal of the instrument response, is given by

$$A_{kl}(f) = S_k(f)L_l(f)G(R)\exp(-\pi f R Q_{Lg}^{-1}/v). \quad (1)$$

where $S_k(f)$ is the source term, $L_l(f)$ is the local site term, R is the hypocentral distance, v is the average *Lg* peak velocity (3.35 km s^{-1}), Q_{Lg} is the quality factor, and $G(R)$ is the geometrical spreading, which is given by [*Herrmann and Kijko*, 1983]

$$G(R) = \begin{cases} R^{-1} & R \le R_x \\ (R_x R)^{-1/2} & R \ge R_x. \end{cases} \quad (2)$$

[13] This form of $G(R)$ implies dominance of body waves for $R \le R_x$ and of surface waves for $R \ge R_x$. *Herrmann and Kijko* [1983] showed that R_x is twice the crustal thickness, which in the region of interest is about 40–45 km. In this study we set R_x to be 100 km. *Shin and Herrmann* [1987] reported that the observed geometrical spreading of *Lg* waves in the time domain, $R^{-0.83}$, is equivalent to $R^{-0.5}$ in the frequency domain. Taking the logarithm of (1) for distances larger than R_x gives

$$\log A_{kl}(f) + 0.5\log(R_x R) = \log S_k(f) + \log L_l(f) - (\pi f R \log(e)/v)Q_{Lg}^{-1}. \quad (3)$$

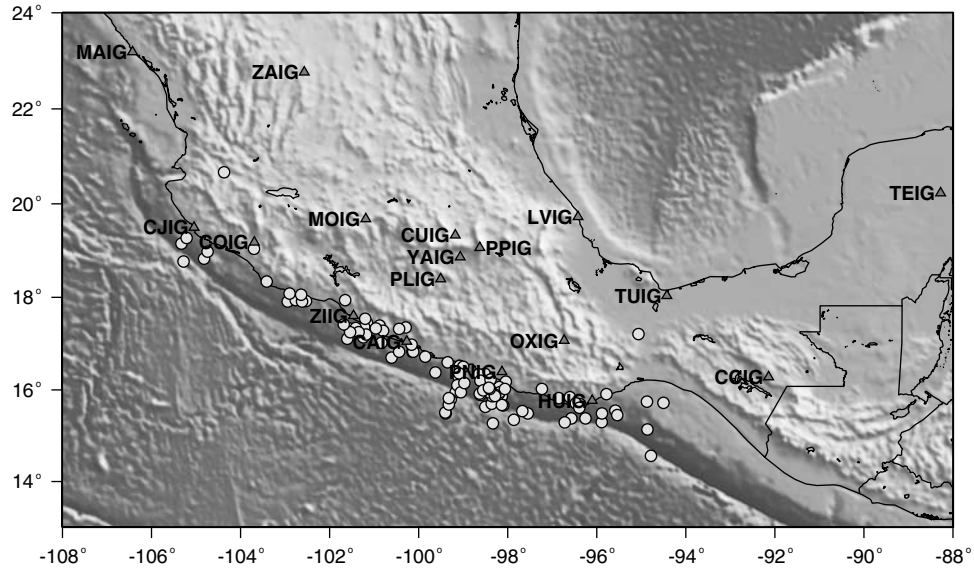

Figure 3. Station (triangles) and epicenter (circles) locations used in this study.

[14] As a constraint for the site terms we required that

$$\sum_{l} \log L_l(f) = 0\,. \tag{4}$$

[15] Equation (3) can be written in matrix formulation as

$$\mathbf{d} = \mathbf{G}\hat{\mathbf{m}}\,, \tag{5}$$

where **d** is the data vector, which is the left hand side of equation (3); **G** is the kernel matrix; and $\hat{\mathbf{m}}$ is the estimated model vector. The estimated model contains the source terms, the site terms, and the average inverse quality factor $Q_{Lg}{}^{-1}$. The linear overdetermined inverse problem was solved through singular value decomposition [*Menke*, 1989; *Press et al.*, 1986].

[16] In the determination of the average Q_{Lg}^{-1}, the inefficient travel paths that are not representative for central southern Mexico were omitted, which means that mostly travel paths from events in the subduction zone west of 96°W were used (Figure 8). The average Q_{Lg}^{-1} was determined for the vertical and horizontal components separately. The horizontal component was taken as square root of the squared spectral amplitudes from the E-W and N-S components. The results did not show any significant differences. The results for Q_{Lg}^{-1} presented here are derived from the vertical components.

[17] The dependence of Q with frequency is generally approximated [e.g., *Fedotov and Boldyrev*, 1969; *Aki*, 1980] by a power law in the form of

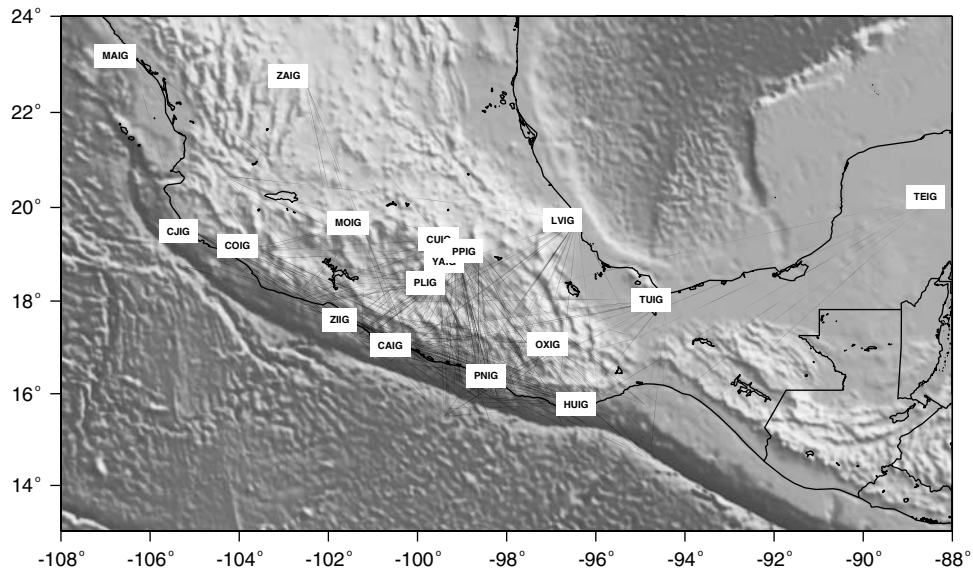

Figure 4. Travel paths showing the complete data set.

$$Q_{Lg}(f) = Q_0 f^{\beta}. \quad (6)$$

[18] The frequency dependence obtained for Q_{Lg}^{-1} is shown in Figure 9. The relation for Q_{Lg}^{-1} in the frequency range 1.6–8 Hz is given by $Q_{Lg}^{-1}(f) = 0.00489\ (\pm 0.0006)\ f^{-0.85\ (\pm 0.089)}$, which corresponds to $Q_{Lg}(f) = 204\ f^{0.85}$. This result, considering the relatively large uncertainties, is in agreement with other studies, for example, *Ordaz and Singh* [1992]. Our result has been obtained from a larger data set and hence is valid for a larger part of southern Mexico. Below 1.6 Hz, Q_{Lg}^{-1} only shows minor changes with frequency and can be approximated by its value at 1.6 Hz. *Aki* [1980], on the basis of the comparison of frequency-dependent Q_S^{-1} at high frequencies (1–25 Hz) and Q^{-1} from surface wave measurements at long periods, postulated that Q_S^{-1} may have a peak value at around 0.5 Hz. Our observations (Figure 9) show a peak of Q_{Lg}^{-1} at around 1 Hz. This is an important result since it gives support to Aki's hypothesis on the basis of the analysis of a single wave type. The frequency dependence of Q_{Lg}^{-1} in the frequency range 1.6–8 Hz is expected to be mainly caused by the frequency dependence of scattering attenuation, while intrinsic attenuation is less frequency dependent [e.g., *Dainty*, 1981; *Mayeda et al.*, 1992].

[19] A difference in the attenuation for paths going parallel to the coast compared with paths going inland was observed by *Singh et al.* [1988] and *Cárdenas et al.* [1998]. To investigate this difference, the data set was divided into two groups of travel paths, parallel and perpendicular to the coast, and inverted for Q_{Lg}^{-1} independently. No significant difference was found. This result

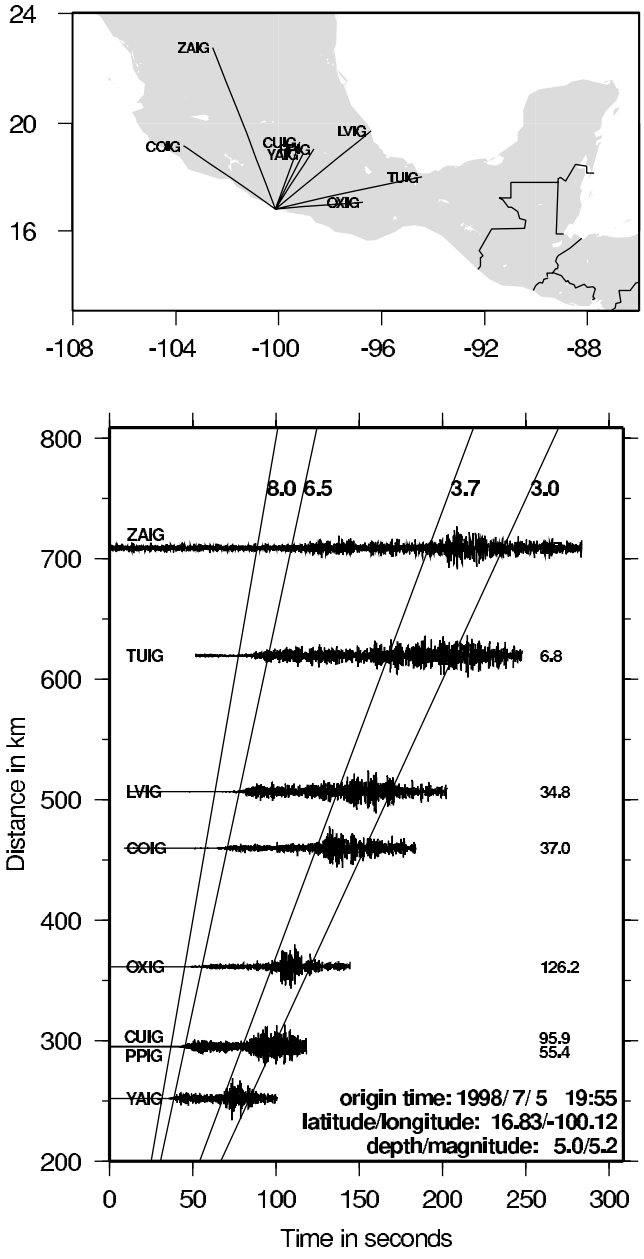

Figure 5. Seismogram distance plots that show *Lg* propagation. The top map shows the travel paths. In the bottom plot, station codes are given on the left, and the numbers on the right side of the traces indicate the *Lg* to *Pn* spectral ratio at 2 Hz. The numbers above the traces and the lines show the group velocity windows. The seismograms are filtered between 1 and 5 Hz.

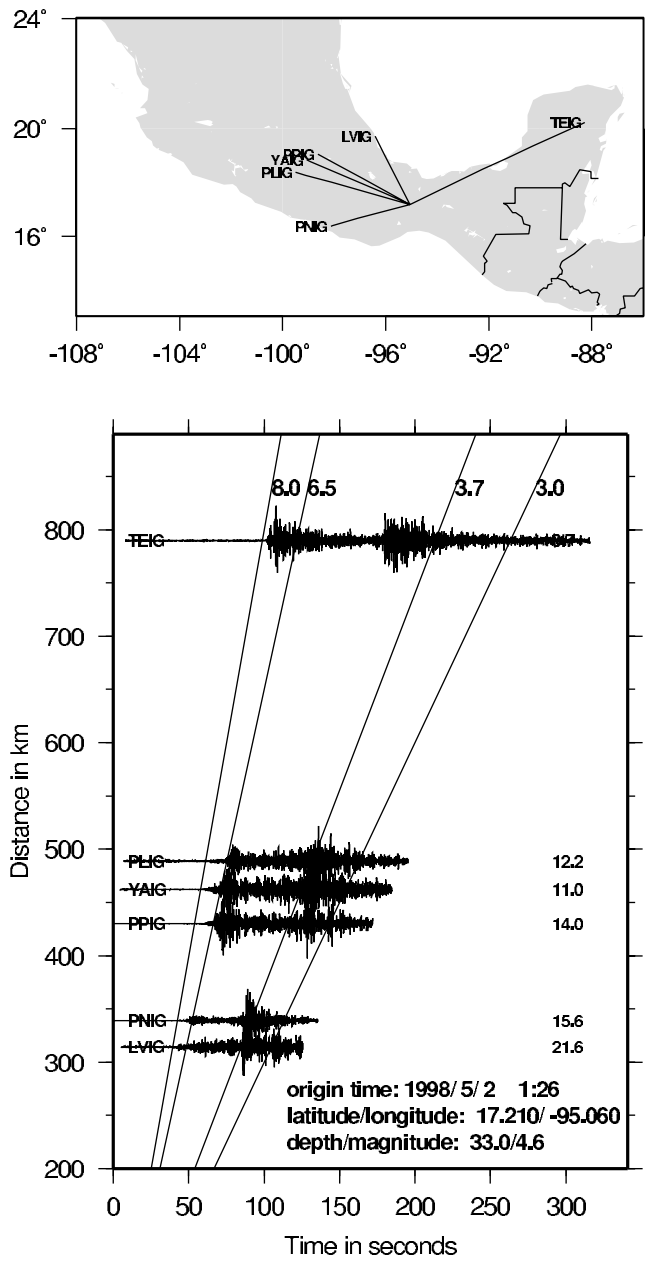

Figure 6. Example of inefficient *Lg* propagation to station TEIG. For details, see Figure 5.

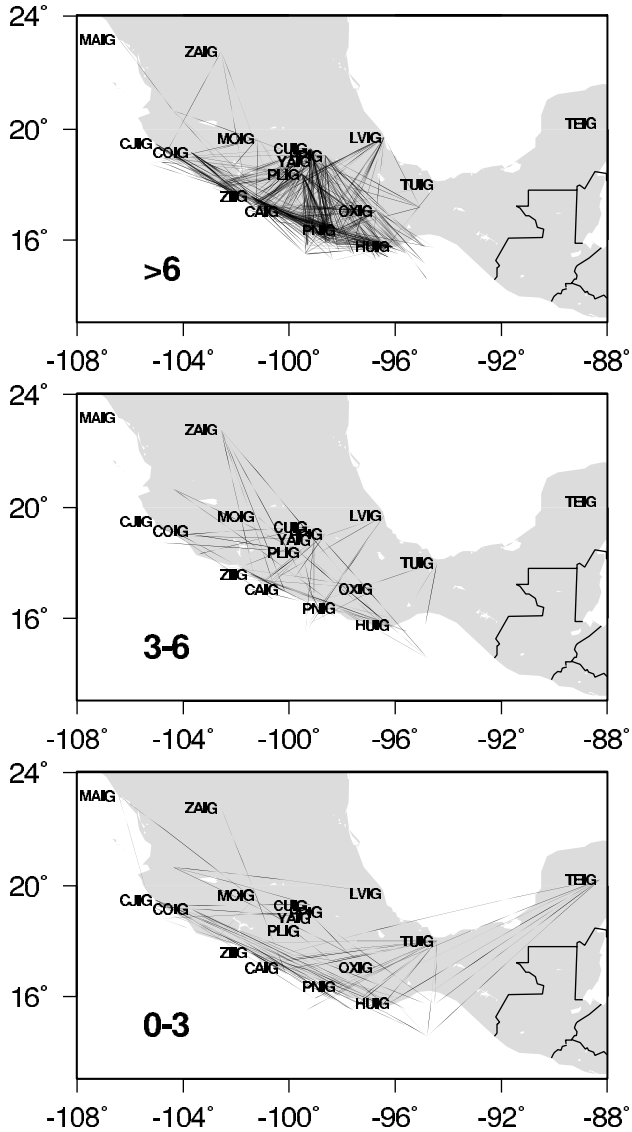

Figure 7. *Lg* propagation efficiency at 2.0 Hz, estimated from *Lg* to *Pn* spectral ratio. The ratio range is given in the bottom left corner of each map. The events are grouped into inefficient ($0 <$ ratio ≤ 3), intermediate ($3 <$ ratio ≤ 6), and efficient (ratio > 6) *Lg* propagation.

means that on a regional scale, there is no evidence of the difference, which may exist on a smaller scale.

5. Q_{Lg} Tomography

[20] A tomography study, based on a large, high-quality data set, can provide valuable information on the lateral variation of the quality factor Q [*Campillo*, 1987; *Baumont et al.*, 1999]. The tomography inverse problem is generally mixed determined; that is, while some model parameters are overdetermined, others are underdetermined [*Menke*, 1989]. Obviously, the problem of Q tomography in southern Mexico is mixed determined, since some areas have a high path coverage, while other areas are poorly covered. We follow the approach presented by *Barmin et al.* [2001], who described a fast and reliable method to solve two-dimensional tomography problems applying simple regularization conditions.

5.1. Method

[21] The area of interest was divided into evenly spaced grid cells with a dimension of 1° in both N-S and E-W directions. Tests with different grid sizes were performed, giving very similar results. The attenuation term for a single travel path is given by $\exp(-\pi f v^{-1}((\Sigma R_i)\, Q_{Lg\ \text{a priori}}{}^{-1} + (\Sigma R_i \Delta Q_{Lg}^{-1})))$ where i is the grid cell index; R_i is the length of the travel path; and $\Delta Q_{Lg\ i}^{-1}$ is the difference from $Q_{Lg\ \text{a priori}}{}^{-1}$, the regional average obtained above, in the grid cell i. Equivalent to (3), we obtain

$$\log A_{kl}(f,R) + 0.5 \log (R_x R) + \pi\Big(\sum R_i\Big) f \log (e) v^{-1} Q_{Lg\ \text{a priori}}^{-1} = \log S_k(f) + \log L_l(f) - (\pi f \log (e) v^{-1}) \sum (Q_{Lg\ i}^{-1} R_i). \quad (7)$$

[22] This system of linear equations again can be written in a matrix formulation as given in (5). The model vector now contains the $\Delta Q_{Lg\ i}^{-1}$ values instead of the average Q_{Lg}^{-1}. The data vector is modified from (3). The function that we minimize is of the form

$$(\mathbf{Gm} - \mathbf{d})^T \mathbf{C_d}^{-1} (\mathbf{Gm} - \mathbf{d}) + \mathbf{m}^T \mathbf{A} \mathbf{m}\,, \quad (8)$$

where $\mathbf{C_d}^{-1}$ is the data covariance matrix, which we set to the identity matrix, $\mathbf{I}$, assuming that our data is uncorrelated. The dimension of the $\mathbf{G}$ matrix is $M \times N$. N is the number of travel paths, M is the number of all model parameters, and Y is the number of the Q_{Lg}^{-1} model parameters. In order to regularize the mixed determined problem the matrix $\mathbf{A}$, with dimension $M \times M$, is added:

$$\mathbf{A} = \mathbf{F}^T \mathbf{F} + \mathbf{H}^T \mathbf{H}\,, \quad (9)$$

[23] The $\mathbf{F}$ matrix adds spatial smoothness for the Q_{Lg}^{-1} model parameters, while $\mathbf{H}$ adds Q_{Lg}^{-1} a priori information for underdetermined grid cells. $\mathbf{F}$ is given as

$$\mathbf{F}_{ij} = \begin{cases} \alpha & i = j \\ -\alpha V_{ij}/p_j & i \neq j, \end{cases} \quad (10)$$

where

$$V_{ij} = \exp\Big(-R_{ij}^2 \Big/ 2\sigma^2\Big) \quad (11)$$

and

$$p_j = \sum_{i=1,\, i\neq j}^{Y} V_{ij}\,. \quad (12)$$

[24] The damping constant α was set to 500 and the spatial smoothing constant σ was set to 100. These values were selected by trial method to produce a smooth tomographic model with recognized tectonic patterns. Because of the $\mathbf{F}$ matrix the differences between spatially near grid cells will be minimized. The $\mathbf{H}$ matrix is defined as

$$\mathbf{H}_{ij} = \begin{cases} 0 & i \neq j \\ \beta \exp(-\lambda L_{ij}) & i = j, \end{cases} \quad (13)$$

where L_{ij} is the sum of all travel path segments crossing the grid cell ij. The damping constant β and the constant λ were set to 1000 and 0.001, respectively. These parameters were selected on the basis of visual analysis of the results, ensuring that the $\mathbf{H}$ matrix

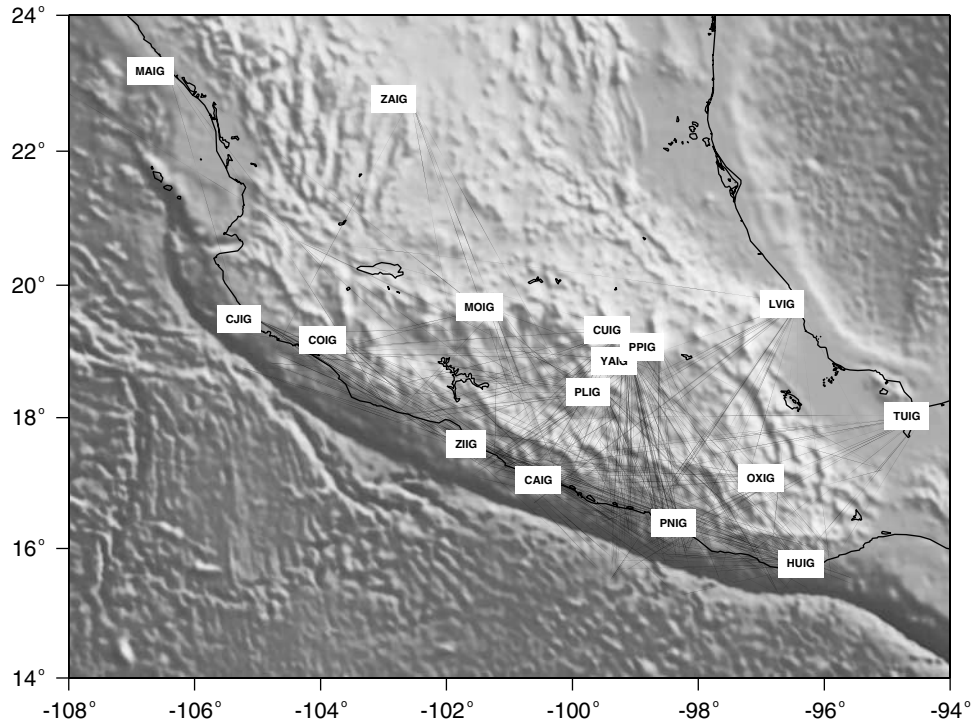

Figure 8. Travel paths showing events and stations used for determining the average inverse quality factor.

adds a priori information only where the travel path coverage is low.

[25] The estimated model vector is obtained through

$$\hat{\mathbf{m}} = \tilde{\mathbf{G}}\mathbf{d} \tag{14}$$

with

$$\tilde{\mathbf{G}} = \left(\mathbf{G}^T\mathbf{G} + \mathbf{A}\right)^{-1}\mathbf{G}^T . \tag{15}$$

[26] The model resolution matrix **R** is given by

$$\hat{\mathbf{m}} = \tilde{\mathbf{G}}\mathbf{d} = \mathbf{G}\tilde{\mathbf{G}}\mathbf{m} = \mathbf{R}\mathbf{m} , \tag{16}$$

where **m** is the true model vector and $\hat{G}$ is given by (15). To estimate the approximate spatial resolution, from each row of the resolution matrix **R** we computed the model spatial resolution for the cell i as

$$\mathbf{m}^i_{\mathrm{SR}} = \left(\sum_{j=1}^{Y} \mathbf{R}_{ij} r_{ij}\right) \Big/ \sum_{j=1}^{Y} r_{ij}, \tag{17}$$

where $\mathbf{R}_{ij}$ is the distance between grid cell i and j and r_{ij} is the element of the resolution matrix.

5.2. Results

[27] In the inversion a tradeoff among Q_{Lg}^{-1}, the site term, and the source term is possible. This may be especially true for travel paths to TEIG, east of 96°W (Figure 7), because of low station coverage in this region. Initial inversions suggested that this was in fact so. For this reason, we fixed the site term at TEIG to 1, while requiring $\Sigma log\ L_i\ (f) = 0$ for the remaining sites. TEIG is a hard limestone site, so that $L(f) = 1$ is reasonable. As shown in Appendix A, the source and the site terms estimated from the inversion are reasonable, giving confidence in our results on Q_{Lg}^{-1}.

[28] The tomography inversion was performed separately for 16 frequencies between 0.2 and 8 Hz. The results for Q_{Lg}^{-1}, the spatial

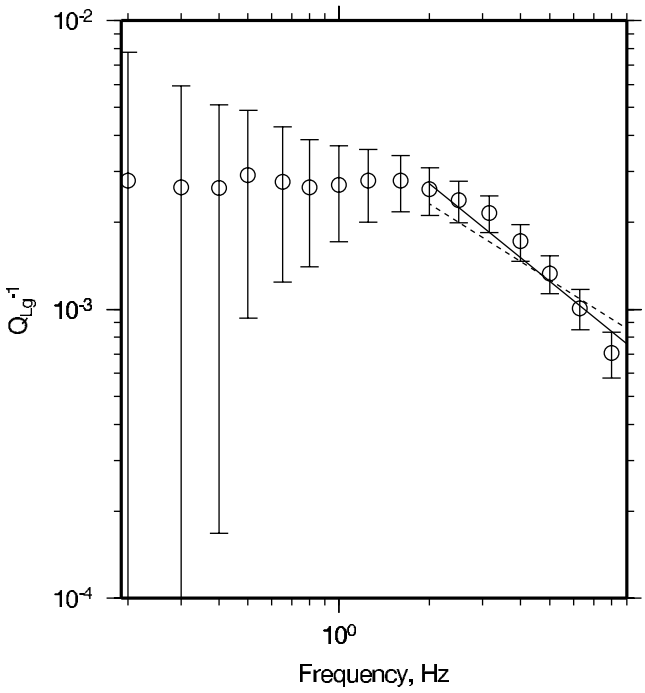

Figure 9. Average inverse quality factor Q_{Lg}^{-1} as a function of frequency; data points obtained shown as circles with error bars corresponding to 1 standard deviation. The solid line is the linear least squares fit using data points between 2 and 8 Hz from this study; the dashed line shows the result of *Ordaz and Singh* [1992].

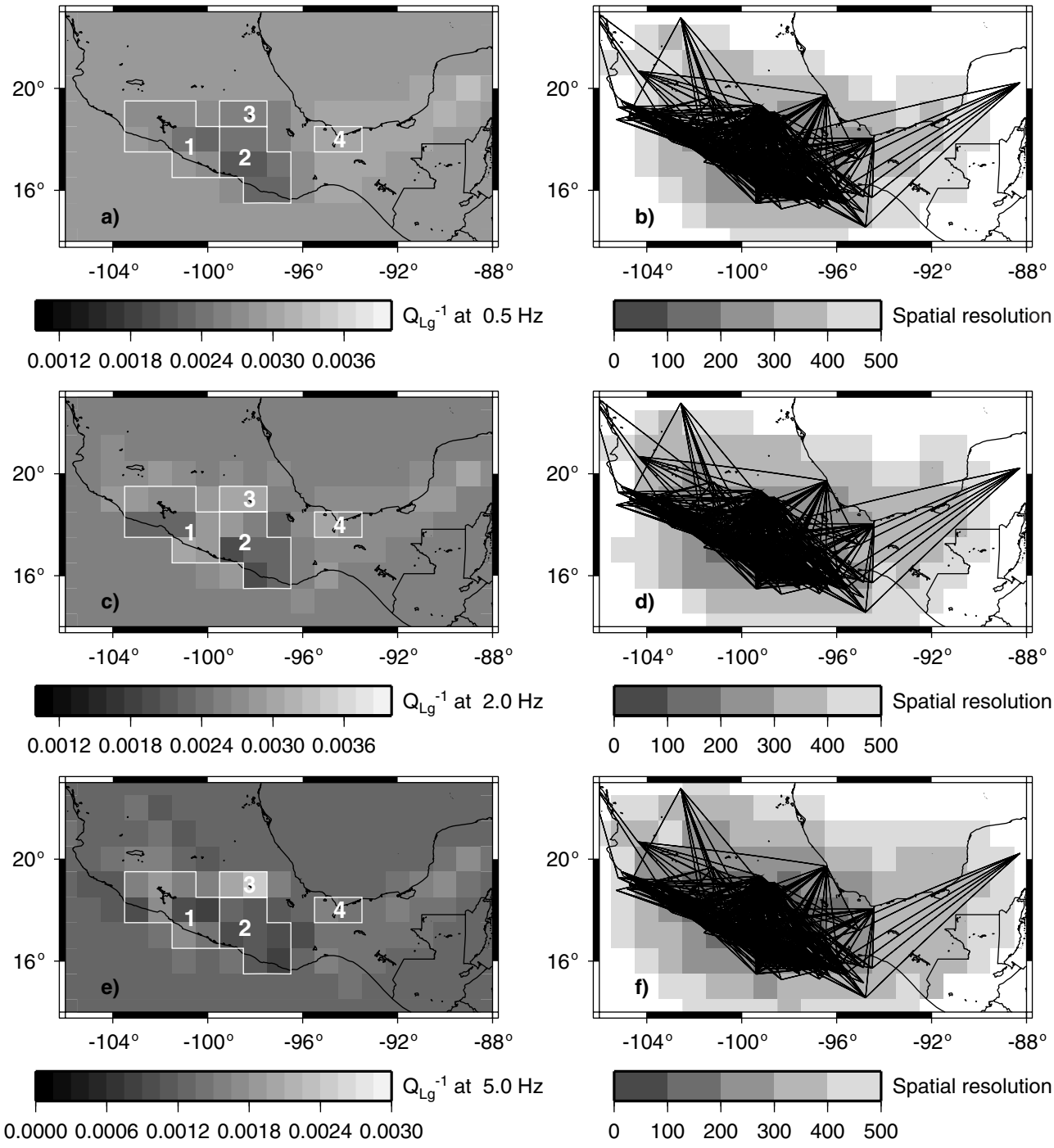

Figure 10. Results from the tomography inversion at various frequencies: (a) Q_{Lg}^{-1} at 0.5 Hz, (c) Q_{Lg}^{-1} at 2.0 Hz, and (e) Q_{Lg}^{-1} at 5.0 Hz. The spatial resolution and the travel paths at the respective frequencies: (b) 0.5 Hz, (d) 2.0 Hz, and (f) 5.0 Hz. The numbers and outlined areas in Figures 10a, 10c, and 10e show the regions defined through variation of Q_{Lg}^{-1}: 1 is Guerrero, 2 is Mixteco-Oaxaca, 3 is Trans-Mexican Volcanic belt (TMVB) near Popocatépetl, and 4 is Gulf coastal plains. The site term at TEIG is fixed to 1.

resolution, and the travel paths used at 0.5, 2.0 and 5.0 Hz are shown in Figure 10. For brevity, the results for the other frequencies, which show similar patterns, are not shown here. The spatial resolution in grid cells with high path coverage is in the range 100–200 km, while it is 200–300 km in the cells with sparse path coverage. This indicates that lateral inhomogeneities with dimension of about 200 km were resolved in the inversion. Areas without or with little path coverage are fixed to the a priori value by the **H** matrix in the inversion. The effect of the smoothing matrix **F** is seen at the boundary between well constrained and unconstrained grid cells.

[29] An additional estimation of the model resolution was obtained through a checkerboard test. In this test a synthetic checkerboard model was used with positive variation from the a priori Q_{Lg}^{-1} value for even grid cells and a negative deviation for odd grid cells. The synthetic data values were computed for the

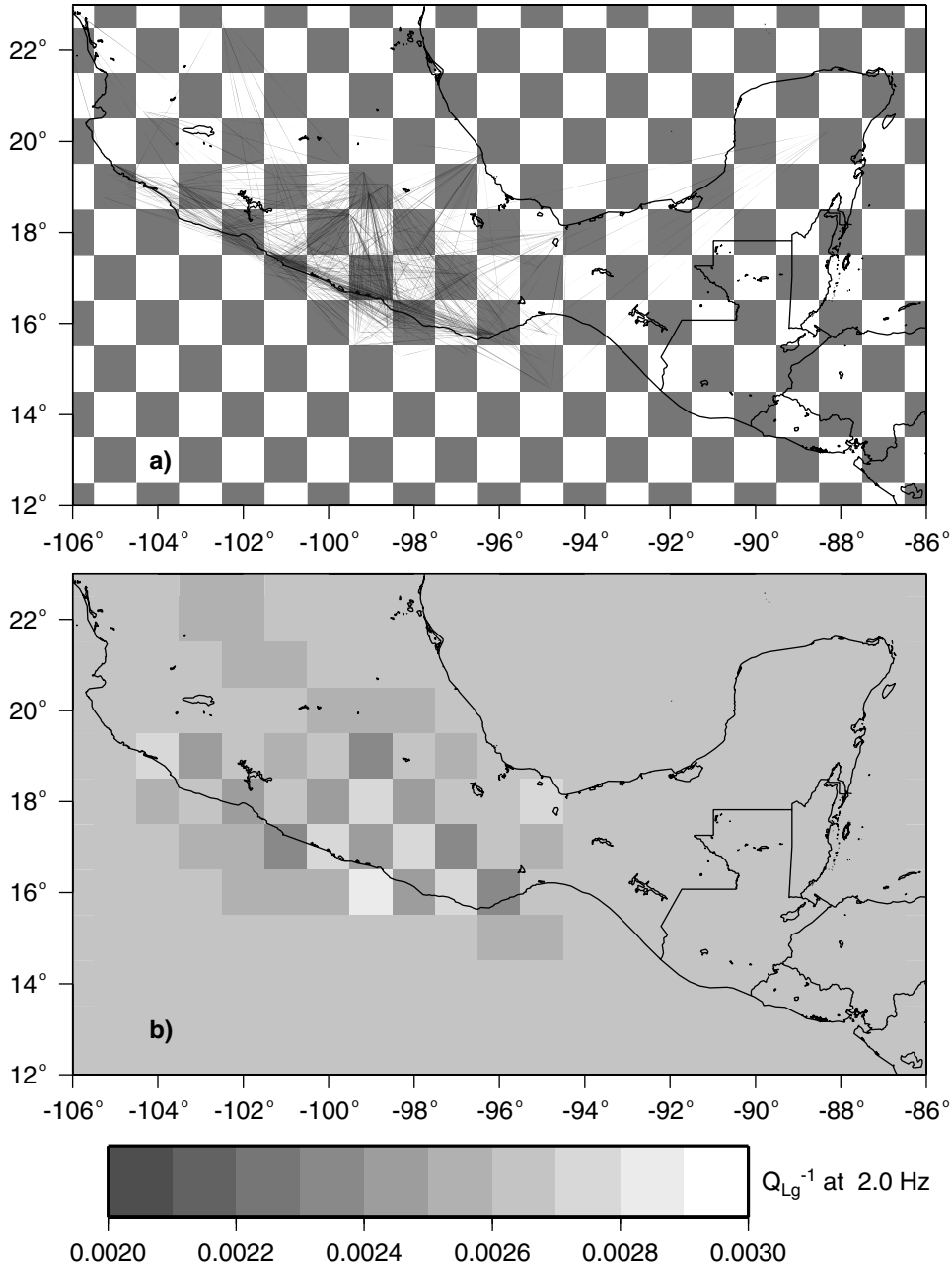

Figure 11. Results from the checkerboard test. The same parameters as in the inversion of the real data were used. (a) Synthetic model with positive and negative deviation from the a priori value and travel paths, which are the same as those used in the inversion of real data at 2 Hz. (b) Result from the inversion of the synthetic data shown in Figure 11a.

same travel paths as used in the inversion of real data (Figure 10). The inversion of the synthetic data was performed with the same damping parameters as used in the inversion of real data. The model vector in the inversion of the synthetic data only included the ΔQ_{Lg}^{-1} parameters. The results from this test are shown in Figure 11. It is seen that the smoothness constraint is reflected in the inverted result, however, the checkerboard pattern is clearly resolved in areas with high path coverage. *Leveque et al.* [1993] have shown that smaller structures like in the checkerboard test can be well retrieved in the tomographic inversion, while larger structures are poorly retrieved. However, we consider this checkerboard test as a minimum requirement, indicating the reliability of our results.

[30] The main tectonic features or lateral variations that were resolved in the Q tomography inversion include the differences between the Mixteco-Oaxaca and the Guerrero terranes, the Trans-Mexican Volcanic Belt (TMVB), and the coastal plain of the Gulf of Mexico. The boundaries of these regions are shown in Figure 10. Because of low path coverage north of 20°N, no difference from the average value was obtained for this region. The average Q_{Lg}^{-1} values obtained as a function of frequency for the various regions are shown in Figure 12, and the linear relationships for Q_{Lg}^{-1} (f) are given in Table 2.

[31] In regions of recent tectonic activity it is reasonable to expect high scattering and hence low Q [*Dainty*, 1981]. For the Mixteco-Oaxaca terrane, higher Q_{Lg} values compared with the

Guerrero terrane were obtained. This result is expected, since the Mixteco-Oaxaca complex is composed of old Precambrian rocks, while the Guerrero terrane has undergone more recent collision tectonics. Previous studies for Guerrero [*Castro et al.*, 1990; *Ordaz and Singh*, 1992] are representatives of the Guerrero terrane, and give similar results to ours. The study by *Castro and Munguía* [1993] for Oaxaca gives smaller Q values for the area 97.2° to 96.3°W and 15.5° to 16.2°N. Low Q values for this region may not be representative for the entire Mixteco-Oaxaca terrane. In our study the resolution in these regions is the highest, which gives us confidence in our results.

[32] Low Q_{Lg} values, corresponding to high attenuation, were obtained in the TMVB close to the Popocatépetl volcano. Figure 12 shows that the difference in Q_{Lg} compared with adjacent regions is more pronounced at higher frequencies. This result is similar to that reported by *Shapiro et al.* [2000]. The strong attenuation at higher frequencies in the volcanic zone is probably caused by heating or partial melting of the crustal material and/or by the enhanced scattering caused by the higher level of small-scale heterogeneities due to the active tectonic processes in the volcanic zone. In the remaining part of the TMVB the spatial resolution was low, but there was indication for low Q_{Lg} values (Figure 10).

[33] Another region where low Q_{Lg} values were observed is the Gulf of Mexico coastal plain. This is in accordance with the analysis of the efficiency of *Lg* propagation. The difference in Q_{Lg} relative to the adjacent regions is more pronounced at low frequencies and disappears above 5 Hz. The fact that the lower Q_{Lg} is observed at low frequencies suggests that the *Lg* attenuation in this region is caused by some structural effect. One possible cause could be the variation in the Moho topography [e.g., *Kennett*, 1986; *Campillo*, 1987; *Campillo et al.*, 1993]. Gravity-based studies [*Wollard et al.*, 1956] show that in the Gulf coastal plain the crust is thinner than in central southern Mexico. However, the numerical simulation of *Lg* propagation in heterogeneous models shows that the variations in Moho topography alone cannot explain the very strong *Lg* attenuation [e.g., *Maupin*, 1989; *Regan and Harkrider*, 1989; *Cao and Muirhead*, 1993]. Another mechanism for the strong *Lg* attenuation is the entrapment of the seismic energy in shallow sedimentary layers [e.g., *Knopoff et al.*, 1979; *Zhang and Lay*, 1995; *Shapiro et al.*, 1996]. This mechanism is more likely to be responsible for the low Q_{Lg} in the Gulf coastal plain.

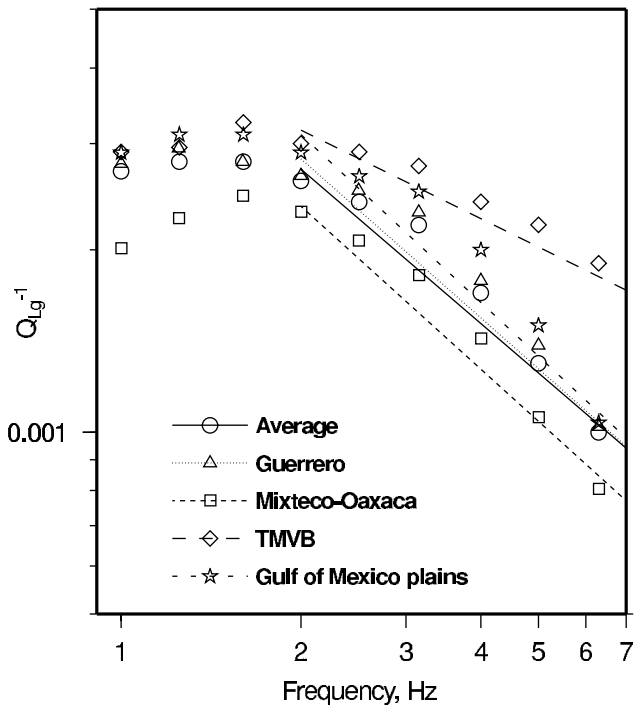

Figure 12. Values of Q_{Lg}^{-1} as a function of frequency for the regions shown in Figure 10.

Table 2. $Q_{Lg}^{-1}(f)$ for Various Regions Obtained in This Study[a]

Region	*a*	*b*
Average	0.00493 ± 0.00063	−0.854 ± 0.089
Guerrero	0.00517 ± 0.00086	−0.872 ± 0.113
Mixteco-Oaxaca	0.00439 ± 0.00049	−0.895 ± 0.077
TMVB	0.00442 ± 0.00042	−0.486 ± 0.067
Gulf of Mexico	0.00587 ± 0.00110	−0.921 ± 0.124

[a] The relationship is given by $Q_{Lg}^{-1}(f) = af^{-b}$.

[34] The study by *Cárdenas et al.* [1998] reported lower Q values for travel paths along the coast as compared with travel paths perpendicular to the coast. This observation seems to agree with the tomography results. In *Cárdenas et al.*'s [1998] study the travel paths along the coast were between 99.5°W and 102°W, and the inland travel paths were from the endpoints toward Mexico City. It is seen that both inland going travel paths propagate in grid cells of higher Q values as compared with the travel path along the coast. Thus their result is explained by local lateral variation of Q. The difference in Q_{Lg}^{-1} was not seen in section 5.1 because it was determined for the entire coastal region.

[35] These results suggest that significant differences in Q_{Lg} are preserved between tectonic units, despite these units being subjected to the ongoing subduction process. It is assumed that in the frequency range below 8 Hz, scattering attenuation is more dominant than anelastic attenuation [*Dainty*, 1981; *Mayeda et al.*, 1992]. It is possible that attenuation in the crust is affected by the subduction process through changes in the thermal regime of the upper plate and the release of fluids from the subducted oceanic crust. It seems, however, that these processes are secondary, and Q_{Lg} mainly reflects scattering attenuation.

6. Conclusions

[36] Our study of *Lg* waves in southern Mexico leads to the following conclusions:

1. *Lg* wave propagation is inefficient in the coastal plains of the Gulf of Mexico and in the Gulf of Tehuantepec.
2. An average Q_{Lg} for efficient travel paths in the frequency range 1.6–8 Hz can be expressed as $Q_{Lg}(f) = 204\, f^{0.85}$.
3. Q_{Lg}^{-1} determined from a single wave type shows a peak value at around 1 Hz.
4. Q_{Lg} for Oaxaca is higher compared with Guerrero, in contradiction to some previous studies.
5. Q_{Lg} is low below Popocatépetl, an active volcano.
6. The coastal plain of the Gulf of Mexico is characterized by low Q_{Lg}.

[37] The results on *Lg* wave propagation show strong correlation with the crustal structure. Inefficient *Lg* wave propagation in the coastal plains of the Gulf of Mexico and the Gulf of Tehuantepec is an expected result owing to the presence of thick sediments in these regions. Higher Q_{Lg} in Oaxaca as compared with Guerrero is explained by the presence of Precambrian, cratonic rocks in the former terrane and prevalence of collision tectonics in the latter terrane. Low Q_{Lg} below the active Popocatépetl volcano is a consequence of partially molten magma and increased scattering.

[38] Table 2 summarizes Q_{Lg}^{-1} for different regions and gives an average value for the regions with efficient *Lg* propagation. This table may be useful in estimation of ground motions from future earthquakes, a task of great importance in Mexico. In

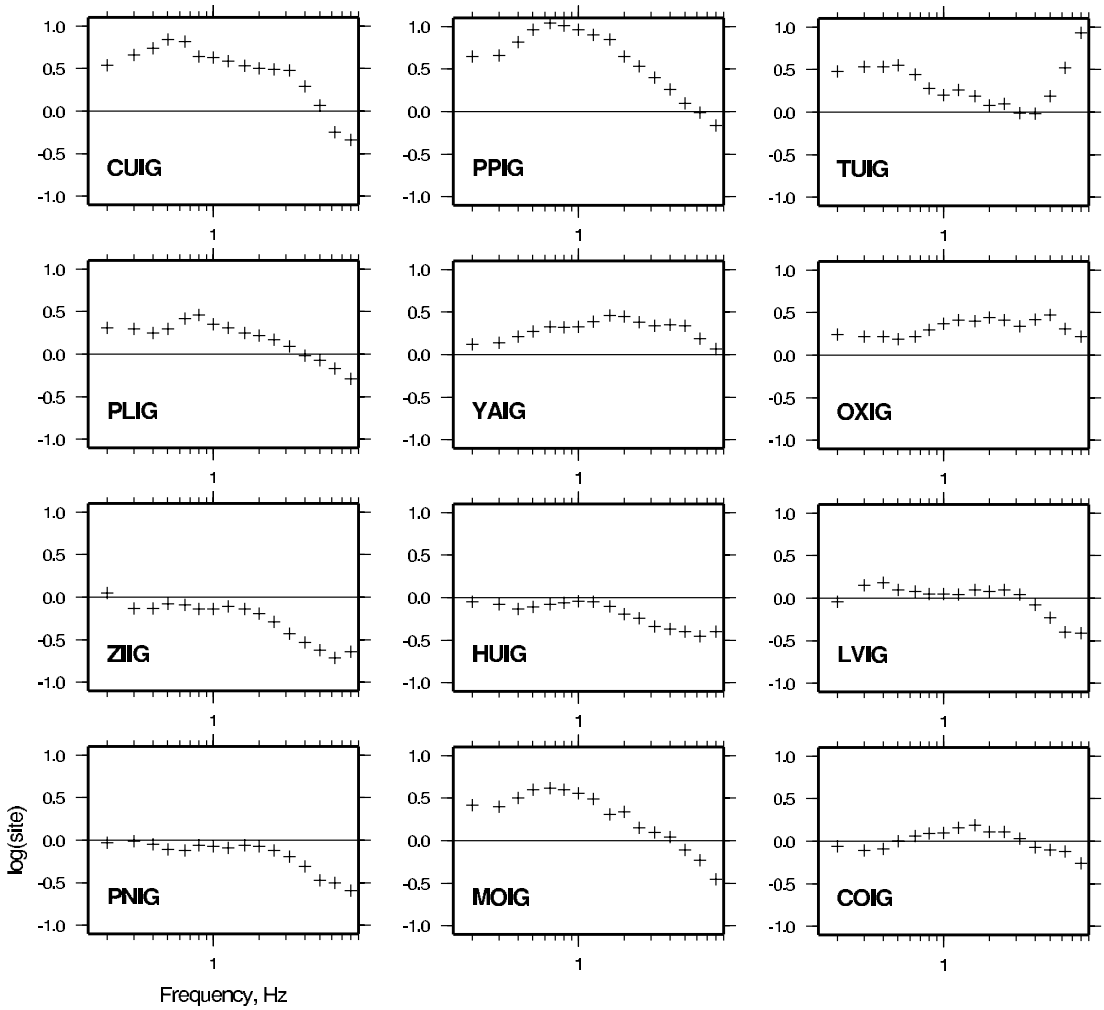

Figure A1. Site terms as obtained in the average Q_{Lg}^{-1} inversion from horizontal components.

some parts of Mexico the spatial resolution was too low to resolve Q. To improve the regional coverage, additional stations are needed, especially for the regions north of 20°N and east of 92°W.

Appendix A

[39] Equations (3) and (9) suggest that there might be a tradeoff among site terms, source terms, and Q_{Lg}^{-1}. To investigate whether this tradeoff is severe, we examined the site terms at each station and the source terms of each event. For this purpose, we used results obtained from the inversion of horizontal components. Figure A1 shows the site terms for selected stations.

[40] The results obtained for the sites CUIG and PPIG, which are located near each other in the Mexican volcanic belt, show large amplification. This result agrees with *Singh et al.* [1995], who reported a maximum amplification of 10 at frequencies between 0.2 and 0.4 Hz for CUIG. For TUIG, high amplification is obtained at high frequencies, which is expected since the station is located on sediments. Little is known about the amplification at the other sites, but the values seem reasonable in view of the local surface geology of the sites.

[41] From the source term, $S(f)$, obtained from the inversion of the horizontal components, we computed the seismic moment, M_0,

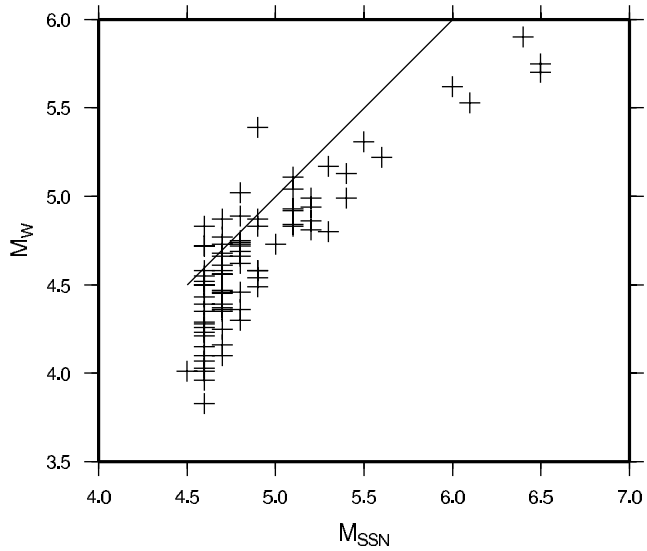

Figure A2. M_W versus M_{SSN}. M_W is computed from the source term obtained from the inversion using horizontal components. M_{SSN} is the magnitude reported by the National Seismological Service (SSN).

assuming a point source dislocation:

$$M_0 = 4\pi\rho\beta^3 S(f \to 0)/(R_{\vartheta\phi} FP) \quad \text{(A1)}$$

where ρ is the density, β is the shear wave velocity, $R_{\vartheta\phi}$ is the average radiation pattern (0.55 [*Boore and Boatwright*, 1984]), F is the free surface amplification (2.0), and P accounts for equal partitioning of energy in the two horizontal components ($(1/\sqrt{2})$). The moment magnitude was computed by [*Kanamori*, 1977]:

$$M_W = 2/3 \log(M_0) - 6.06\,, \quad \text{(A2)}$$

where M_0 is in newton meters. Figure A2 compares M_W obtained from the source term and the magnitude M_{SSN}, reported by the SSN, which is based on the amplitude of long-period (15 to 30 s) waves [*Singh and Pacheco*, 1994]. From Figure A2 we note that (1) M_W is, generally, less than M_{SSN}, and (2) the difference increases for larger earthquakes. Both points 1 and 2 can be explained by the fact that M_W has been estimated at a period of 5 s, while M_{SSN} is based on much longer-period waves.

[42] From Figures A1 and A2 we conclude that site and source terms, retrieved from the inversion, are reasonable, and no serious tradeoff has occurred between them and Q_{Lg}^{-1}.

[43] **Acknowledgments.** Discussions with Bob Herrmann and Michel Campillo are highly appreciated. We are also grateful to Anatoliy Levshin and Mikhail Barmin for their help with the tomography inversion. The review comments by Steve Myers and two anonymous reviewers have been valuable for improvement of the manuscript and are appreciated. This study was carried out while L. O. was at UNAM on a travel grant provided by the Faculty of Natural Sciences and the Institute of Solid Earth Physics, University of Bergen. This research was partially supported by CONACYT (Mexico) projects J32308-T, 27623-T, and G25842-T and DGAPA (UNAM) projects IN109598 and IN105199.

References

Aki, K., Attenuation of shear-waves in the lithosphere for frequencies from 0.05 to 25 Hz, *Phys. Earth Planet. Inter.*, *21*, 50–60, 1980.

Barmin, M. P., M. H. Ritzwoller, and A. L. Levshin, A fast and reliable method for surface wave tomography, *Pure Appl. Geophys.*, *158*, 1351–1375, 2001.

Baumgardt, D. R., Investigation of teleseismic *Lg* blockage and scattering using regional arrays, *Bull. Seiemol. Soc.*, *80*, 2261–2281, 1990.

Baumont, D., A. Paul, S. Beck, and G. Zandt, Strong crustal heterogeneity in the Bolivian Altiplano as suggested by attenuation of *Lg* waves, *J. Geophys. Res.*, *104*, 20,287–20,305, 1999.

Benz, H. M., A. Frankel, and D. M. Boore, Regional *Lg* attenuation for the continental United States, *Bull. Seismol. Soc. Am.*, *87*, 606–619, 1997.

Boore, D. M., and J. Boatwright, Average body-wave radiation coefficient, *Bull. Seismol. Soc. Am.*, *74*, 1615–1621, 1984.

Calvert, A., E. Sandvol, D. Seber, M. Barazangi, F. Vidal, G. Alguacil, and N. Jabour, Propagation of regional seismic phases (*Lg* and *Sn*) and *Pn* velocity structure along the Africa Iberia plate boundary zone: Tectonic implications, *Geophys. J. Int.*, *142*, 384–408, 2000.

Campa, M. F., and P. J. Coney, Tectono-stratigrafic terranes and mineral resource distributions in Mexico, *Can. J. Earth Sci.*, *20*, 1040–1051, 1983.

Campillo, M., *Lg* wave propagation in a laterally varying crust and the distribution of the apparent quality factor in Central France, *J. Geophys. Res.*, *92*, 12,604–12,614, 1987.

Campillo, M., Propagation and attenuation characteristics of the crustal phase Lg, *Pure Appl. Geophys.*, *132*, 1–19, 1990.

Campillo, M., and J. L. Plantet, Frequency dependence and spatial distribution of seismic attenuation in France: Experimental results and possible interpretations, *Phys. Earth Planet. Inter.*, *67*, 48–64, 1991.

Campillo, M., M. Bouchon, and B. Massinon, Theoretical study of the excitation, spectral characteristics, and geometrical attenuation of regional seismic phases, *Bull. Seiesmol. Soc. Am.*, *74*, 79–90, 1984.

Campillo, M., B. Feignier, M. Bouchon, and N. Béthoux, Attenuation of crustal waves across the Alpine Range, *J. Geophys. Res.*, *98*, 1987–1996, 1993.

Campillo, M., S. K. Singh, N. Shapiro, J. Pacheco, and R. B. Herrmann, Crustal structure south of the Mexican volcanic belt, based on group velocity dispersion, *Geofís. Int.*, *35*, 361–370, 1996.

Cao, A., and K. J. Muirhead, Finite difference modelling of *Lg* blockage, *Geophys. J. Int.*, *115*, 85–96, 1993.

Cárdenas, M., F. Núñez-Cornú, J. Lermo, D. Córdoba, and A. Gonzáles, Seismic energy attenuation in the region between the coast of Guerrero and Mexico City: Differences between paths along and perpendicular to the coast, *Phys. Earth PLanet. Inter.*, *105*, 47–57, 1998.

Castro, R. R., and L. Munguía, Attenuation of *P* and *S* waves in the Oaxaca, Mexico, subduction zone, *Phys. Earth Planet. Inter.*, *76*, 179–187, 1993.

Castro, R. R., J. G. Anderson, and S. K. Singh, Site response, attenuation and source spectra of *S* waves along the Guerrero, Mexico, subduction zone, *Bull. Seismol. Soc. Am.*, *80*, 1481–1503, 1990.

Castro, R. R., L. Munguía, C. J. Rebollar, and J. Acosta, A comparative analysis of the quality factor *Q* for the regions of Guerrero and Oaxaca, Mexico, *Geofís. Int.*, *33*, 373–383, 1994.

Chazalon, A., M. Campillo, R. Gibson, and E. Carreno, Crustal wave propagation anomaly across the Pyrenean Range: Comparison between observations and numerical simulations, *Geophys. J. Int.*, *115*, 829–838, 1993.

Dainty, A., A scattering model to explain seismic *Q* observations in the lithosphere between 1 and 30 Hz, *Geophys. Res. Lett.*, *8*, 1126–1128, 1981.

Domínguez, T., C. J. Rebollar, and R. R. Castro, Regional variations of seismic attenuation of *Lg* waves in southern Mexico, *J. Geophys. Res.*, *102*, 27,501–27,509, 1997.

Fedotov, S. A., and S. A. Boldyrev, Frequency dependence of the body-wave absorption in the crust and the upper mantle of the Kuril-island chain, *Izv. Acad. Sci. USSR Solid Earth*, *11*, 553–562, 1969.

Fix, J. E., The crust and upper mantle of central Mexico, *Geophys. J. R. Astron. Soc.*, *43*, 453–500, 1975.

Furumura, T., and B. L. N. Kennett, On the nature of regional seismic phases, II, On the influence of structural barriers, *Geophys. J. Int.*, *129*, 221–234, 1997.

Furumura, T., and B. L. N. Kennett, On the nature of regional seismic phases, III, The influence of crustal heterogeneity on the wavefield for subduction earthquakes: The 1985 Michoacan and 1995 Copala, Mexico earthquakes, *Geophys. J. Int.*, *135*, 1060–1084, 1998.

Gibson, R. L., and M. Campillo, Numerical simulations of high- and low-frequency *Lg* wave propagation, *Geophys. J. Int.*, *118*, 47–56, 1994.

Gomberg, J. S., and T. G. Masters, Waveform modelling using locked mode synthetics and differential seismograms: Application to determination of the structure of Mexico, *Geophys. J. R. Astron. Soc.*, *94*, 193–218, 1988.

Gregersen, S., and F. Vaccari, *Lg*-wave modelling for the North Sea, *Geophys. J. Int.*, *114*, 76–80, 1993.

Guzman, E., Sedimentary volumes in gulf coastal plain of United States and Mexico, part V, Volumes of mesozoic and cenozoic sediments in Mexican gulf coastal plain, *Geol. Soc. Am. Bull.*, *63*, 1200–1220, 1962.

Hasegawa, H. S., *Lg* spectra of local earthquakes recorded by the Eastern Canada telemetered network and spectral scaling, *Bull. Seismol. Soc. Am.*, *73*, 1041–1061, 1983.

Herrmann, R. B., and A. Kijko, Modeling some empirical vertical component *Lg* relations, *Bull. Seismol. Soc. Am.*, *73*, 157–171, 1983.

Kanamori, H., The energy release in great earthquakes, *J. Geophys. Res.*, *82*, 1981–1987, 1977.

Kennett, B. L. N., *Lg* waves and structural boundaries, *Bull. Seismol. Soc. Am.*, *76*, 1133–1141, 1986.

Kennett, B. L. N., S. Gregersen, S. Mykkeltveit, and R. Newmark, Mapping of crustal heterogeneities in the North Sea Basin via the propagation of *Lg* waves, *Geophys. J. R. Astron. Soc.*, *83*, 299–306, 1985.

Knopoff, L., R. G. Mitchel, E. G. Kausel, and F. Schwav, A search for the oceanic *Lg* phase, *Geophys. J. R. Astron. Soc.*, *56*, 211–218, 1979.

Leveque, J.-J., L. Rivera, and G. Wittlinger, On the use of the checker-board test to assess the resolution of tomographic inversions, *Geophys. J. Int.*, *115*, 313–318, 1993.

Maupin, V., Numerical modelling of *Lg* wave propagation across the North Sea, *Geophys. J. Int.*, *99*, 273–283, 1989.

Mayeda, K., S. Koyanagi, M. Hoshiba, K. Aki, and Y. Zeng, A comparative study of scattering, intrinsic, and coda Q^{-1} for Hawaii, Long Valley, and Central California between 1.5 and 15.0 Hz, *J. Geophys. Res.*, *97*, 6643–6659, 1992.

McNamara, D. E., T. J. Owens, and W. R. Walter, Propagation characteristics of *Lg* across the Tibetan Palteau, *Bull. Seismol. Soc. Am.*, *86*, 457–469, 1996.

Mellors, R. J., V. E. Camp, F. L. Vernon, A. M. S. Al-Amri, and A. Chalib, Regional waveform propagation in the Arabian Peninsula, *J. Geophys. Res.*, *104*, 20,221–20,235, 1999.

Menke, W., *Geophysical Data Analysis: Discrete Inverse Theory, Int. Geophys. Ser.*, vol. 45, 289 pp., Academic, San Diego, Calif., 1989.

Meyer, R. P., J. S. Steinhart, and G. P. Woollard, Central Plateau, Mexico, in *Explosion Studies of Continental Structure*, edited by J. S. Steihart and R. P. Meyer, *Carnegie Inst. Washington Publ.*, *622*, 199–225, 1961.

Nava, F. A., Structure of the Middle America Trench in Oaxaca, Mexico, *Tectonophysics*, *154*, 241–255, 1988.

Ordaz, M., and S. K. Singh, Source spectra and spectral attenuation of seismic waves from Mexican earthquakes, and evidence of amplification in the hill zone of Mexico City, *Bull Seismol. Soc. Am.*, *82*, 24–43, 1992.

Press, F., and M. Ewing, Two slow surface waves across North America, *Bull. Seismol. Soc. Am.*, *42*, 219–228, 1952.

Press, W. H., B. P. Flannery, S. A. Teukolsky, and W. T. Vetterling, *Numerical Recipes*, 702 pp., Cambridge Univ. Press, New York, 1986.

Regan, J., and D. G. Harkrider, Numerical modeling of SH *Lg* waves in and near continental margins, *Geophys. J. Int.*, *98*, 107–130, 1989.

Rial, J. A., and M. H. Ritzwoller, Characteristics of *Lg* propagation across South America, *Geophys. J. Int.*, *131*, 401–408, 1997.

Rodgers, A. J., J. F. Ni, and T. M. Hearn, Propagation characteristics of short-period *Sn* and *Lg* in the Middle East, *Bull. Seismol. Soc. Am.*, *87*, 396–413, 1997.

Ruzaikin, A., I. L. Nersesov, and V. I. Khalturin, Propagation of *Lg* and lateral variations in the crustal structure in Asia, *J. Geophys. Res.*, *82*, 307–316, 1977.

Sedlock, R. L., F. Ortga-Gutiérrez, and R. C. Speed, Tectonostratigraphic terranes and tectonic evolution of Mexico, *Geol. Soc. Am. Spec. Pap.*, *278*, 1993.

Shapiro, N., N. Béthoux, M. Campillo, and A. Paul, Regional seismic phases across the Ligurian Sea: *Lg* blockage and oceanic propagation, *Phys. Earth Planet. Inter.*, *93*, 257–268, 1996.

Shapiro, N. M., M. Campillo, A. Paul, S. K. Singh, D. Jongmans, and F. J. Sanchez-Sesma, Surface wave propagation across the Mexican Volcanic belt and the Origin of the long-period seismic-wave amplification in the Valley of Mexico, *Geophys. J. Int.*, *128*, 151–166, 1997.

Shapiro, N. M., S. K. Singh, A. Iglesias-Mendoza, V. M. Cruz-Atienza, and J. F. Pacheco, Evidence of low *Q* below Popocatepetl volcano and its implication to seismic hazard estimation in Mexico City, *Geophys. Res. Lett.*, *27*, 2753–2756, 2000.

Shi, J., W.-Y. Kim, and P. G. Richards, Variability of crustal attenuation in the northeastern United States from *Lg* waves, *J. Geophys. Res.*, *101*, 25,231–25,242, 1996.

Shin, T.-C., and R. B. Herrmann, Lg attenuation and source studies using 1982 Miramichi data, *Bull. Seismol. Soc. Am.*, *77*, 384–397, 1987.

Singh, S., and R. B. Herrmann, Regionalization of crustal coda *Q* in the continental United States, *J. Geophys. Res.*, *88*, 527–538, 1983.

Singh, S. K., and J. Pacheco, Magnitude of Mexican earthquakes, *Geofis. Int.*, *33*, 189–198, 1994.

Singh, S. K., E. Mena, and R. R. Castro, Some aspects of source characteristics of the 19 September 1985 Michoacan earthquake and ground motion amplification in and near Mexico City from strong motion data, *Bull Seismol. Soc. Am.*, *78*, 451–477, 1988.

Singh, S. K., R. Quaas, M. Ordaz, F. Mooser, D. Almora, M. Torres, and R. Vásquez, Is there truly a "hard" rock site in the Valley of Mexico?, *Geophys. Res. Lett.*, *22*, 481–484, 1995.

Vaccari, F., and S. Gregersen, Physical description of *Lg* waves in inhomogeneous continental crust, *Geophys. J. Int.*, *135*, 711–720, 1998.

Valdés, C. M., W. D. Mooney, S. K. Singh, R. P. Meyer, C. Lomnitz, J. H. Luetgert, B. T. Helsley, B. T. R. Lewis, and M. Mena, Crustal structure of Oaxaca, Mexico from seismic refraction measurements, *Bull. Seismol. Soc. Am.*, *76*, 547–564, 1986.

Wollard, G. P., and J. Monges Caldera, Gravedad, Geologia regional y estructura cortical en México, *Anales Inst. Geofís. 2*, 60 pp., Univ. Nac. Auton. Mex., Mexico City, 1956.

Xie, J., and J. Mitchell, A back-projection method for imaging large-scale lateral variations of *Lg* coda *Q* with application to continental Africa, *Geophys. J. Int.*, *100*, 161–181, 1990.

Yamamoto, J., L. Quintanar, R. B. Herrmann, and C. Fuentes, Lateral variation of *Lg* coda *Q* in southern Mexico, *Pure Appl. Geophys.*, *149*, 575–599, 1997.

Zhang, T. R., and T. Lay, Why the *Lg* phase does not traverse oceanic crust, *Bull. Seismol. Soc. Am.*, *85*, 1665–1678, 1995.

L. Ottemöller, British Geological Survey, Murchison House, West Mains Road, Edinburgh EH9 3LA, UK. (lot@bgs.ac.uk)

J. F. Pacheco, N. M. Shapiro, and S. K. Singh, Instituto de Geofísica, Universidad Nacional Autónoma de México, Ciudad University, 04510 México City, DF, Mexico.

N. M. Shapiro, Center for Imaging Earth's Interior, Department of Physics, University of Colorado, Campus Box 390, Boulder, CO 80309-0390, USA. (nshapiro@anquetil.colorado.edu)